Journal of Energy Storage 51 (2022) 104386

Contents lists available at ScienceDirect

Journal of Energy Storage

journal homepage: www.elsevier.com/locate/est

Research papers

Artificial neural network-Genetic algorithm optimized graded metal foam

K. Venkateshwar [a,*], S.H. Tasnim [a], S.A. Gadsden [b], S. Mahmud [a]

[a] School of Engineering, University of Guelph, Guelph, Ontario N1G 2W1, Canada
[b] Department of Mechanical Engineering, McMaster University, Hamilton, Ontario L8S4L8, Canada

ARTICLE INFO

Keywords:
Artificial neural network
Design optimization
Genetic algorithm
Metal foam
Thermal energy storage

ABSTRACT

The effective utilization of renewable energy directly correlates to efficient performance of integrated energy storage system. The efficiency of Thermal Energy Storage (TES) systems strongly correlates with the heat transfer rate during phase change processes. Heterogeneous metal foams which allow augmenting heat transfer without compromising the thermal capacity suffers from high manufacturing cost. A series of homogeneous metal foams stacked is employable to reap advantages associated with heterogeneous metal foam at a similar manufacturing cost as homogeneous metal foam. The present study focuses on optimizing the porosity distribution of graded metal foam to augment the performance of the TES system. The unidirectional phase change process, observed particularly during solidification, acts as a bottleneck. Therefore, the present study focuses on augmenting unidirectional phase-change processes. The present study discusses the influence of PCM and metal foam thermophysical properties and operational characteristics of the TES system on heat transfer augmentation in different graded metal foams. A numerical model is developed to quantify the influence of graded metal foam on heat transfer rate, which is used to train an Artificial Neural Network (ANN) model. The porosity distribution has been optimized using a Genetic algorithm, which employs the ANN model to ascertain heat transfer rate for different graded metal foams. The optimal distribution has been found to be 93.7% and 96.3% for two-layer graded metal foam and 92.8%, 95%, and 97.2% for three-layer graded metal foam, which augments heat transfer by 1160% and 1185%, respectively.

1. Introduction

Thermal Energy Storage (TES) is vital for building thermal management, waste heat recovery, and efficient utilization of renewable energy resources [1,2]. The high energy density, low cost, and durability make Phase Change Materials (PCMs) ideal for TES application. However, the intrinsic low thermal conductivity of PCMs poses a significant challenge, as it reduces efficiency and increases charging and discharging time [3]. Therefore, in the past two decades, significant effort has been dedicated to augmenting the effective thermal conductivity of PCMs [4,5]. Among several approaches proposed and analyzed, the impregnation of PCM in metal foams has proved to be highly efficient [6]. However, the addition of metal foam reduces the volume available for the PCM, hence reducing the capacity of TES systems [7]. Therefore, the recent focus has been to achieve heat transfer augmentation with limited compromise in the thermal energy storage capacity. One of the approaches is to employ heterogeneous metal foam [8–17].

Yang et al. [8] experimentally analyzed unidirectional solidification in the presence of metal foams of different porosities, materials, and pore densities, stacked together in different orientations. Yang et al. [9] numerically analyzed the influence of heterogeneous metal foam with linearly varying porosity. Kumar and Saha [10] numerically studied phase change inside shell and tube heat exchanger in the presence of heterogeneous metal foam. Tao et al. [11] numerically studied the progress of melt fraction inside homogeneous metal foam and two different porosity metal foams stacked together. Zhang and He [12] numerically studied the melting of paraffin in heterogeneous metal foam with linearly varying porosity. Venkateshwar et al. [13] studied the solidification of *n*-octadecane impregnated in five different heterogeneous metal foam morphologies. Mahdi and Nsofor [14] numerically studied melting inside shell and tube heat exchanger with three different metal foams arranged radially. Wang et al. [15] experimentally studied melting inside shell and tube with metal foams of four different porosities arranged radially. These studies showed that heterogeneous metal foams with spatial porosity variation such that higher effective thermal conductivity is near boundary surface yields higher heat transfer rate than homogeneous metal foams of similar mean porosities. However, the optimal spatial porosity variation has not been discussed in the literature, limiting the effective utilization of heterogeneous metal

* Corresponding author.
E-mail address: venkatek@uoguelph.ca (K. Venkateshwar).

https://doi.org/10.1016/j.est.2022.104386
Received 24 October 2021; Received in revised form 15 February 2022; Accepted 6 March 2022
Available online 11 March 2022
2352-152X/© 2022 Elsevier Ltd. All rights reserved.

Nomenclature

C_p	Sensible Heat Capacity (J·kg^{-1}·K^{-1})
f_l	Melt Fraction
h_{sf}	Latent Heat Capacity (J·kg^{-1})
k	Thermal Conductivity (W·m^{-1}·K^{-1})
L	Length of the TES system (m)
MRE	Mean Relative Error
MSE	Mean Square Error
N_i	Number of units in ith layer of ANN model
n	Number of segments of Graded Metal Foam
q	Heat flux (W·m^{-2})
$\overline{q}$	Mean Heat Flux (W·m^{-2})
R^2	Absolute fraction of variance
T	Temperature (K)
t	Time (s)

Greek symbol

ε	Porosity
ρ	Density (kg·m^3)

Subscript

ANN	Artificial Neural Network
eff	PCM-Metal foam composite effective
l	Liquid
mf	Metal foam
m	Melting
num	Numerical
PCM	Phase Change Material
s	Solid

foams. Moreover, the high cost associated with manufacturing heterogeneous metal foams limits their application because of economic infeasibility. The challenge associated with the high cost of manufacturing heterogenous metal foam is answerable by employing multiple homogenous metal foams of different porosities arranged to perform as heterogenous metal foam [8,11,14,15]. This allows achieving a higher heat transfer rate without compromising the thermal energy storage capacity. Moreover, the graded metal foam allows achieving a higher heat transfer rate at the same cost as homogeneous metal foam, as the manufacturing process and material quantify remains the same. Therefore, the present study aims to optimize graded metal foam porosity distribution to augment the heat transfer rate.

The optimization of heterogenous metal foam is challenging because of the non-linear dependence of heat transfer rate on porosity distribution, limiting the application of several conventional optimization techniques, requiring non-conventional approaches. Yang et al. [18] optimized graded metal foam morphology to augment phase change process inside shell and tube heat exchanger, using exhaustive search technique. The exhaustive search technique requires analyzing phase change in all plausible graded metal foam morphology, which is computationally expensive. Moreover, the application of conventional optimization techniques based on the gradients is limited because of non-linear nature of the problem. Therefore, Genetic algorithms have been employed to optimize the performance of heat exchangers, HVAC systems, and thermal energy conversion systems [19]. Recently, Genetic algorithm has also been employed for augmenting phase change processes [20]. However, the major challenge associated with employing stochastic optimization techniques is the need to compute the heat transfer rate for various distribution of porosities of graded metal foam while exploring the solution domain, which is computationally expensive. Therefore, it is essential to develop models to estimate the mean heat transfer rate [21,22]. Baby and Balaji used experimental results for melting of PCM in presence of metal fins to train neural network and used it in conjugation with Genetic algorithm for optimization. Kadiyala and Chattopadhyay [22] employed Genetic algorithm in conjugation with Artificial Neural Network to optimize the location of heat sources for optimizing heat transfer.

The present study employs an Artificial Neural Network (ANN) to estimate the heat transfer rate for different graded metal foams. The influence of different graded metal foams on heat transfer characteristics has been numerically calculated to train the ANN model. The intrinsic low thermal conductivity of PCMs poses a significant challenge during the unidirectional phase change process, as conduction is the dominant mode of heat transfer. Therefore, the graded metal foam has been optimized for the unidirectional phase change process in the present study, as it acts as a bottleneck for TES system efficiency. The unidirectional phase change process is observed during solidification, melting with the hot surface on top, and melting with slight differences in boundary and melting temperatures. The robustness of the ANN model to estimate the heat transfer rate has been discussed. Furthermore, the universal application of optimized graded metal foam has been discussed, i.e., the influence of thermophysical properties of PCM and metal foam and operating conditions on optimized graded metal foam has been discussed.

2. Modeling

A mathematical model based on the Enthalpy Porosity method [23] has been developed to analyze phase change in a graded metal foam. Fig. 1 shows the schematic diagram of the TES system. The graded metal foam is composed of three homogeneous metal foams of different porosities. An isothermal cold boundary is placed at the bottom, and other walls are assumed to be adiabatic.

2.1. Numerical modeling

The phase change process is modeled based on the Enthalpy-Porosity technique and the following set of assumptions:

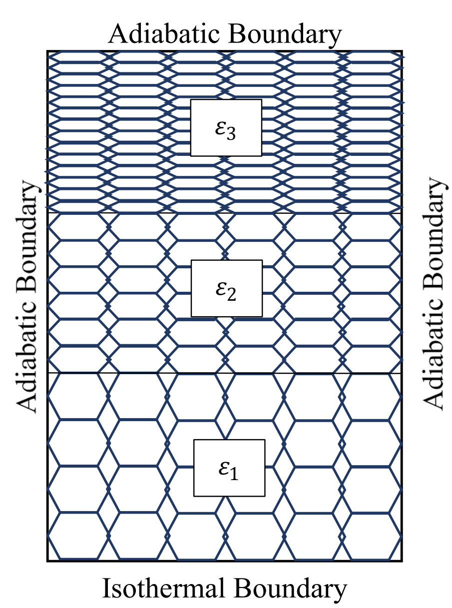

Fig. 1. Schematic diagram of TES system exposed to Isothermal boundary.

(a) Phase Transition occurs at a constant temperature.
(b) Thermophysical properties are temperature independent.
(c) Thermophysical properties in the mushy zone are linearly dependent upon the melt fraction.
(d) The phase change process is unidirectional.

The governing equation is given by [23]:

$$\frac{\partial(\rho_{eff}C_{ps,eff}T)}{\partial t} = \nabla\bullet(\mathrm{k_{eff}}\nabla \mathrm{T}) - \frac{\partial(\mathrm{f_l}\rho_{eff}\mathrm{h_{sf,eff}})}{\partial t} - \frac{\partial\left[\mathrm{f_l}\rho_{eff}(\mathrm{C_{pl,eff}} - \mathrm{C_{ps,eff}})(\mathrm{T}-\mathrm{T_m})\right]}{\partial t}, \tag{1}$$

where, ρ_{eff} is effective density of metal foam-PCM composite, $C_{ps,\ eff}$ is effective sensible heat capacity in solid-state, $C_{pl,\ eff}$ is effective sensible heat capacity in the liquid state, $h_{sf,\ eff}$ is effective latent heat capacity, k_{eff} is effective thermal conductivity, T_m is the phase transition temperature, and f_l is the melt fraction. The effective thermophysical properties of PCM-metal foam are computed as [7,24]:

$$\rho_{eff} = \varepsilon\rho_{PCM} + (1-\varepsilon)\rho_{mf}, \tag{2}$$

$$C_{ps,eff} = \left[\varepsilon\rho_{PCM}C_{ps,PCM} + (1-\varepsilon)\rho_{mf}C_{ps,mf}\right]/\rho_{eff}, \tag{3}$$

$$C_{pl,eff} = \left[\varepsilon\rho_{PCM}C_{pl,PCM} + (1-\varepsilon)\rho_{mf}C_{ps,mf}\right]/\rho_{eff}, \tag{4}$$

$$h_{sf,eff} = \varepsilon\rho_{PCM}h_{sf}/\rho_{eff} \tag{5}$$

$$k_{l,eff} = A\left[\varepsilon k_{l,PCM} + (1-\varepsilon)k_{mf}\right] + (1-A)/\left[\varepsilon/k_{l,PCM} + (1-\varepsilon)/k_{mf}\right], \tag{6}$$

$$k_{s,eff} = A\left[\varepsilon k_{s,PCM} + (1-\varepsilon)k_{mf}\right] + (1-A)/\left[\varepsilon/k_{s,PCM} + (1-\varepsilon)/k_{mf}\right] \tag{7}$$

The numerical modeling and validation have been extensively discussed in [7]. The mean heat flux ($\overline{q}$) during solidification is calculated as

$$\overline{q} = \frac{\int_0^L \rho_{eff}\left[h_{sf,eff}(x) + C_{pl,eff}(x)\{T_h - T_m\} + C_{ps,eff}(x)\{T_m - T(x)\}\right]dx}{t_s}, \tag{8}$$

where, t_s is solidification time, A is the cross-sectional area of the TES system, and L is the length of the TES system.

2.1.1. *Validation*

Figs. 2 and 3 show the time-step and grid size independence analysis, respectively. A time-step of 0.01 s and grid size of 0.1 mm has been used in the present study.

The numerical model has been validated using experimental findings reported by Feng et al. [25] (Fig. 4).

2.2. *Parameter influencing optimization*

The heat transfer characteristics during phase change of PCM impregnated in metal foam depend upon thermophysical properties of PCM and metal foam and operating conditions of the TES system. Therefore, it is essential to analyze the parameters influencing the optimized porosity distribution of graded metal foam.

The two characteristics of the TES system which influence the heat transfer process are dimension and boundary condition. The increase in the length of the TES system reduces the mean heat transfer rate because of a decrease in temperature gradient [7]. The temperatures are bound by phase transition temperature and isothermal boundary temperature, whereas the mean distance between them increases with an increase in the length, thus reducing the mean heat transfer rate. However, the effect of an increase in length of the TES system on the mean heat transfer rate is similar irrespective of the porosity distribution of metal foam. Fig. 5 shows that the enhancement in mean heat transfer rate upon the addition of graded metal foam is independent of the length of the TES system.

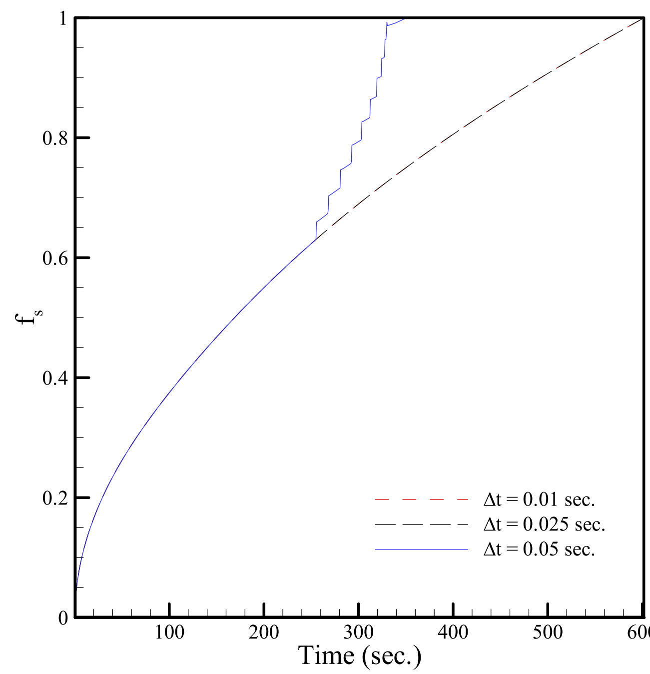

Fig. 2. Time-Step independence analysis.

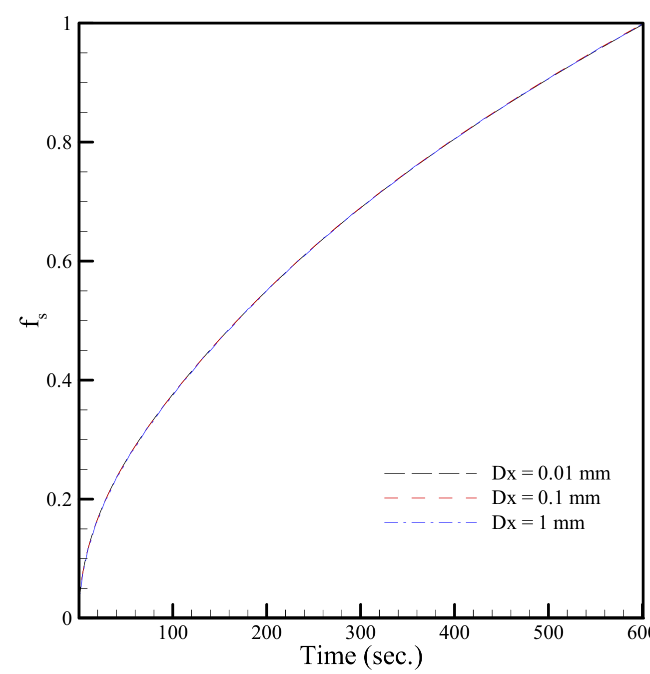

Fig. 3. Grid size independence analysis.

The increase in the difference in the boundary temperature and phase transition temperature increases the mean heat transfer rate. However, the augmentation in the heat transfer rate by increasing the difference between boundary and phase transition temperature is by a similar factor irrespective of metal foam morphology, as evident from Fig. 6. Therefore, optimized graded metal foam morphology is independent of boundary conditions and the length of the TES system.

The latent heat capacity of PCM influences the energy capacity of the TES system and thus the phase change duration, while it has an insignificant influence on the mean heat transfer rate [7]. Therefore, latent heat capacity has an insignificant influence on mean heat transfer

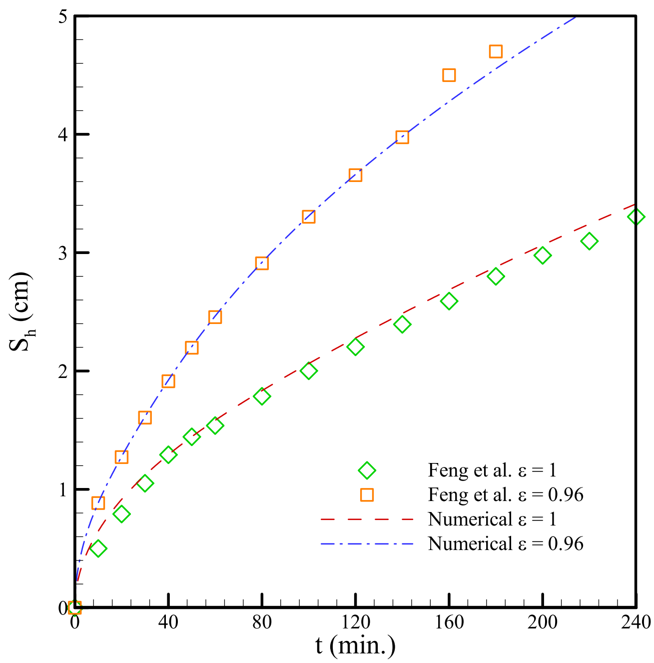

Fig. 4. Validation of numerical model using experimental results reported by Feng et al. [25].

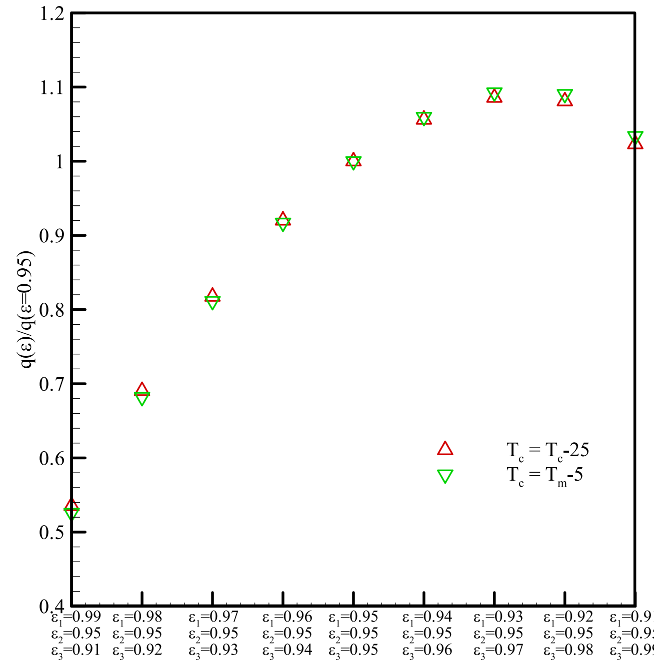

Fig. 6. Influence of isothermal boundary temperature on mean heat transfer enhancement in the presence of different graded metal foams.

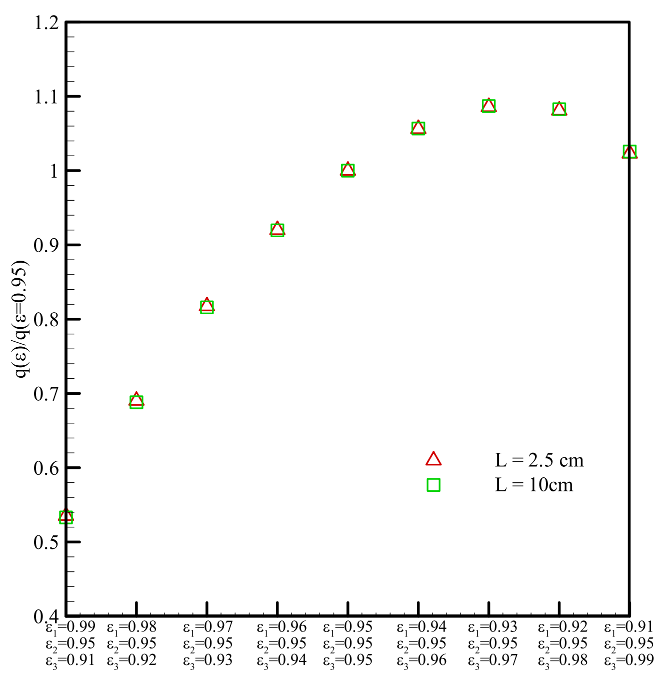

Fig. 5. Influence of length of TES system on mean heat transfer enhancement in the presence of different graded metal foams.

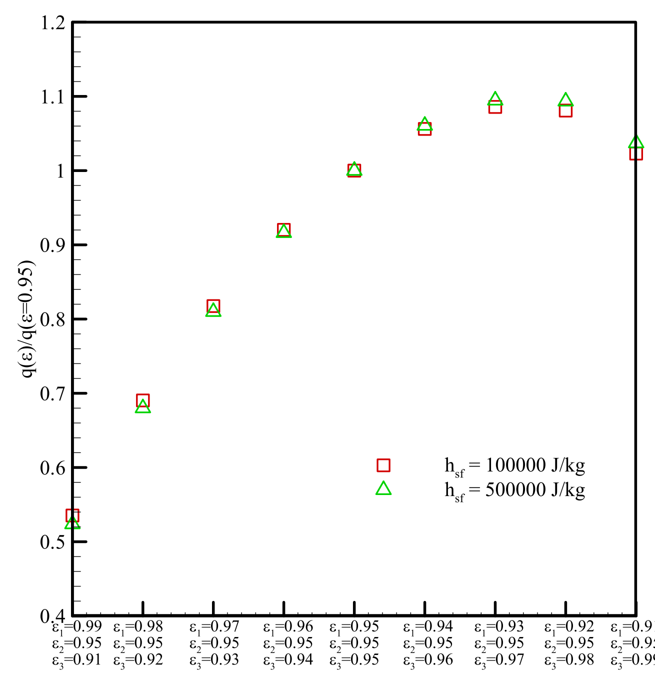

Fig. 7. Influence of latent heat capacity of PCM on mean heat transfer enhancement in the presence of different graded metal foams.

enhancement in the presence of different graded metal foams, as observed in Fig. 7.

The effective thermal conductivity of PCM-metal foam composite directly influences the mean heat transfer rate [7]. The effective thermal conductivity depends upon the thermal conductivities of metal foam and PCM and the porosity of metal foam. Therefore, it is essential to understand the influence of thermal conductivities of metal foam and PCM on heat transfer enhancement in the presence of graded metal foams. The thermal conductivity of PCM studied in the literature varies in the range between 0.25 $W{\cdot}m^{-1}{\cdot}K^{-1}$ and 1 $W{\cdot}m^{-1}{\cdot}K^{-1}$, particularly organic PCMs [3]. Copper and aluminum are the two most commonly studied metal foams, whose conductivity varies in the range between 200 $W{\cdot}m^{-1}{\cdot}K^{-1}$ and 500 $W{\cdot}m^{-1}{\cdot}K^{-1}$ [6]. Fig. 8 shows that the influence of porosity distribution on heat transfer enhancement for metal foam-PCM composite with $k_{PCM} = 0.25$ and 1.00 $W{\cdot}m^{-1}{\cdot}K^{-1}$ and $k_{mf} = 200$ and 500 $W{\cdot}m^{-1}{\cdot}K^{-1}$. Although the values of heat transfer enhancement for PCM-metal foam composites are different, the pattern is similar, and the point of inflection coincides. Therefore, the optimal porosity distribution of graded metal foam will be similar for all combinations of thermal conductivities of metal foam and PCM.

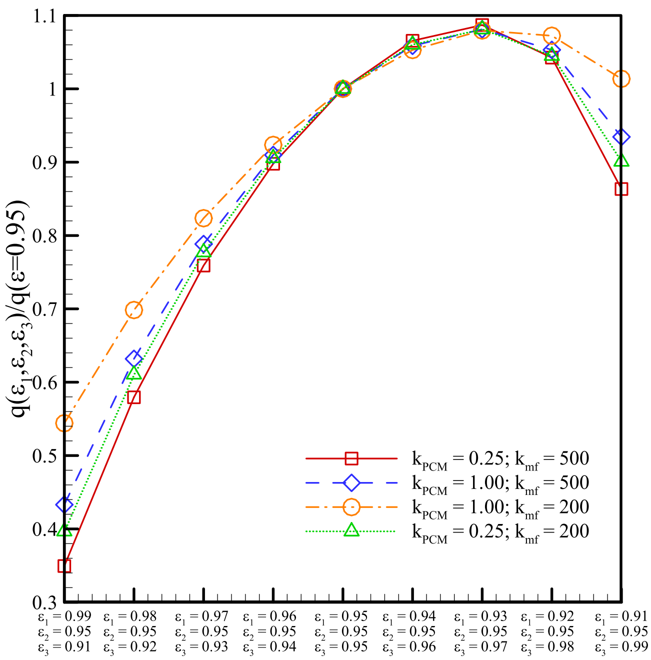

Fig. 8. Influence of thermal conductivities of PCM and metal foam on mean heat transfer enhancement in the presence of different graded metal foams.

The optimal porosity distribution of metal foam for the unidirectional phase change process is similar, irrespective of the boundary temperature, length of the TES system, the latent heat capacity of PCM, and thermal conductivities of commonly used metal foam and organic PCMs. Therefore, in the present study, optimal graded metal foam morphology has been computed employing *n*-octadecane ($k_{PCM,s}$=0.358 W·m^{-1}·K^{-1}) as PCM and aluminum (k_{mf}= 218 W·m^{-1}·K^{-1}) as metal foam. The thermophysical properties of *n*-octadecane and aluminum has been mentioned in Table 1.

2.3. Artificial neural network

Artificial Neural Network (ANN) was developed to estimate the output which involves non-linear combination of input parameters, which are computationally challenging for regression. Fig. 9 shows a representational schematic of an ANN model. ANN receives input parameters and assign different weights to compute values upon which non-linear activation functions are applied to compute vaues for intermediate layers (known as hidden layers), and further uses these values to predict the output value.

A back-propagation feed-forward neural network has developed in the present study. The input layer consists of N_1 units, including the bias unit, equal to the number of segments of graded metal foams (*n*). The mean porosity condition binds the porosity of nth metal foam. Therefore, the input layer consists of information regarding n-1 porosities and a bias unit. The number of units in the hidden layer (N_2) is varied, and the model's performance is analyzed. The sigmoid function is employed as an activation function in the present study. The output layer has a single

Table 1
Thermophysical Properties of PCM and Metal foam.

Properties	n-octadecane		Al
	Solid	Liquid	
ρ	770		2700
k	0.358	0.148	218
C_p	1934	2196	902
T_m	301.16		–
h_{sf}	243,500		–

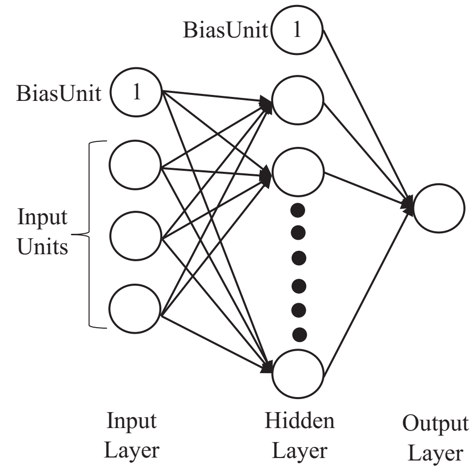

Fig. 9. Representational schematic diagram of artificial neural network.

unit, i.e., heat transfer rate. A scaling factor has been utilized to keep the value of the output layer within the range of 0 and 1, as the value of the sigmoid function is bound by these two limits. Numerical analysis has been conducted for different graded metal foams using the numerical model developed in MATLAB. The dataset is divided with 80% data in the training set and the remaining 20% in the test set.

The Mean Relative Error (MRE), Mean Square Error (MSE), and absolute fraction of variance (R^2) are computed to analyze the robustness of the model, using the following correlations:

$$MRE = \frac{1}{n}\sum_{i=1}^{n}\frac{|\overline{q}_{ANN} - \overline{q}_{num}|}{\overline{q}_{num}}, \tag{9}$$

$$MSE = \frac{1}{n}\sum_{i=1}^{n}(\overline{q}_{ANN} - \overline{q}_{num})^2, \tag{10}$$

$$R^2 = 1 - \left[\frac{\sum_{i=1}^{n}(\overline{q}_{ANN} - \overline{q}_{num})^2}{\sum_{i=1}^{n}(\overline{q}_{num})^2}\right], \tag{11}$$

where, $\overline{q}_{ANN}$ and $\overline{q}_{num}$ are mean heat transfer rates estimated by the ANN model and numerically calculated, respectively. The robustness of the ANN model has been discussed in the "Result and Discussion" section.

2.4. Genetic algorithm

The genetic algorithm employs a stochastic technique for search and works with the binary coding of parameters rather than the parameters themselves. The porosity of open-cell metal foams typically varies between 88% and 100%, i.e., in the range of 12%. The resolution of the optimized porosity distribution is decided to be 0.1%, as a preliminary numerical study shows the limited influence of porosity change of less than 0.1% on heat transfer characteristics. Therefore, a 7- bit binary is required to represent each parameter. The genetic Algorithm model has been developed with elite characteristics, i.e., the parameter yielding the highest mean heat transfer rate is directly carried to the next iteration without undergoing cross-over and mutation. The probability of selection of each parameter for the reproduction stage is computed based on the output it yields. The selected parameters undergo single-point cross-over.

3. Results and discussion

The neural network model was trained to estimate the mean heat transfer rate in the presence of different graded metal foams for *n*-

octadecane. The neural network model was employed by a Genetic algorithm to compute the mean heat transfer rate for various graded metal foams.

Table 2 shows the MRE, MSE, and R^2 calculated using Eqs. (9)–(11), respectively, for different hidden units for graded metal foam with two segments. 15 hidden units have been selected for estimating the heat transfer rate for different graded metal foams with two segments. The optimal porosity distribution computed using the Genetic algorithm is $\varepsilon_1 = 93.7\%$ and $\varepsilon_2 = 96.3\%$, where ε_1 is close to the Isothermal boundary. The impregnation of optimized graded metal foam increases heat transfer rate by approximately 1160% in contrast to 1080% augmentation upon the addition of homogeneous metal foam. Therefore, the mean heat transfer rate in the presence of optimized graded metal foam is approximately 6.75% higher than the homogeneous metal foam of the same mean porosity, i.e., 0.95. Therefore, just employing two homogeneous metal foams of different porosities stacked together augments the heat transfer rate by 6.75% compared to single homogeneous metal foam. This heat transfer augmentation is particularly of interest because there is no adverse effect of a decrease in thermal capacity or increase in cost associated with this approach.

Figs. 10 and 11 show the heat transfer rate and progress of solidification height with time, respectively, in the presence of optimized graded metal foam and homogeneous metal foam. The heat transfer rate (q) is computed as

$$q = -k_{eff}\frac{dT}{dx}\bigg|_{x=0} \tag{12}$$

Fig. 10 shows that the heat transfer rate is higher initially in optimized graded metal foam because of higher effective thermal conductivity near the isothermal boundary in the graded metal foam. However, as solidification progress and the solid-liquid interface moves beyond the mid-way of the TES system, the effective thermal conductivity is lower in graded metal foam owing to higher porosity. Therefore, towards the completion of the phase change process, the instantaneous heat transfer rate is higher in a homogeneous metal foam. Nevertheless, the initial higher heat transfer rate in graded metal foam yields a 6.75% higher mean heat transfer rate.

Fig. 11 shows the progress of solidification height with time is initially higher in optimized graded metal foam, whereas it is vice-versa towards completion of the solidification process. The porosity of graded metal foam close to isothermal boundary is less than that of homogenous metal foam, thus graded metal foam have lower volumetric thermal capacity near isothermal boundary. The lower volumetric thermal capacity accompanied with higher heat transfer rate leads to faster progress of solidification height in graded metal foam initially compared to homogeneous metal foam. As the solidification progresses, the porosity of graded metal foam increases, thus increasing the volumetric thermal capacity and reducing effective thermal conductivity. The reduced heat transfer rate and increased volumetric thermal capacity reduces the progress of solidification height in graded metal foam towards the completion of solidification process, as observed in Fig. 11. The higher solidification rate initially leads to completion of solidification process in approximately 5.5% less time in optimized graded metal foam than uniform metal foam.

Table 2
Results of neuron independence test for 2 segment graded metal foam.

Number of units in hidden layer	MRE	MSE	R^2
12	0.0128	0.000041833	0.9961
13	0.0093	0.000037755	0.9987
14	0.0126	0.000039906	0.9960
15	**0.0092**	**0.000037200**	**0.9987**
16	0.0119	0.000043015	0.9965
17	0.0123	0.000038634	0.9961
18	0.0126	0.000039829	0.9961
19	0.0128	0.000041533	0.9961
20	0.0127	0.000040539	0.9960
21	0.0124	0.000039008	0.9961
22	0.0124	0.000041184	0.9962
23	0.0121	0.000037721	0.9962
24	0.0126	0.000040942	0.9961

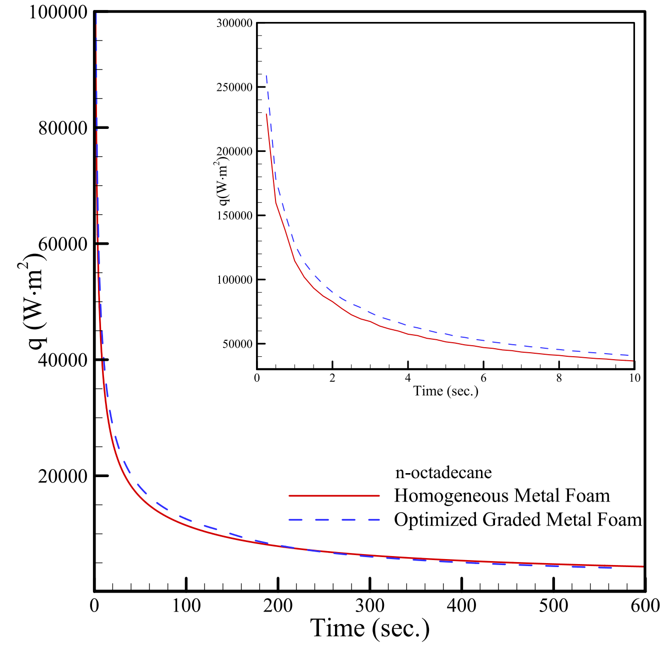

Fig. 10. Heat Transfer rate of TES system filled with n-octadecane in the presence of homogeneous and optimized 2-segment graded metal foams having mean porosity of 0.95.

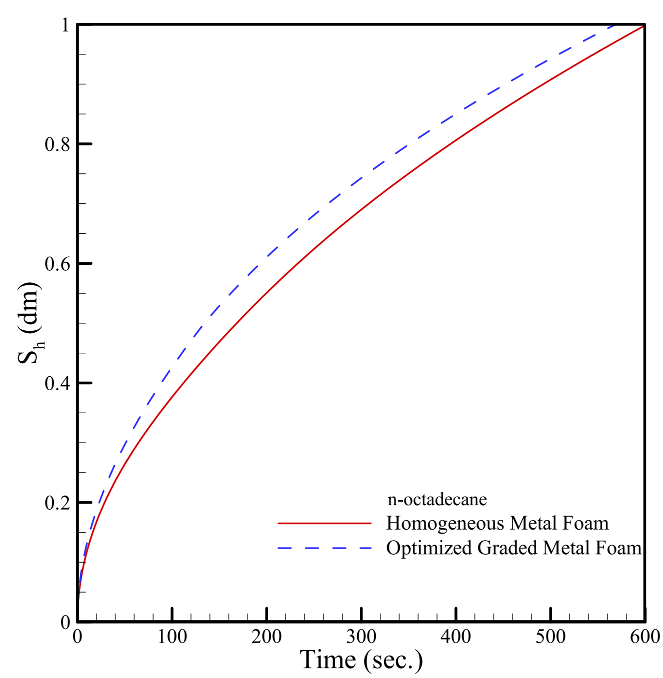

Fig. 11. The progress of solidification height of *n*-octadecane in presence of homogenous and optimized 2-segment graded metal foams respectively.

Table 3 shows the MRE, MSE, and R^2 computed for different hidden units for metal foams with three segments. A hidden layer with 16 units has been selected for estimating the heat transfer rate in the presence of graded metal foam. The optimal porosity distribution is $\varepsilon_1 = 92.8\%$, $\varepsilon_2 = 95.0\%$, and $\varepsilon_3 = 97.2\%$, with ε_1 being closest to the isothermal wall as

Table 3
Results of neuron independence test for 3 segment graded metal foam.

Number of units in hidden layer	MRE	MSE	R^2
10	0.283	0.00092411	0.9678
11	0.0227	0.00034081	0.9841
12	0.0202	0.00019133	0.9879
13	0.0279	0.00033711	0.9779
14	0.0215	0.00020112	0.9876
15	0.0259	0.00027088	0.9823
16	**0.0182**	**0.00016168**	**0.9894**
17	0.0191	0.00016401	0.9889
18	0.0208	0.00018189	0.988
19	0.0257	0.00026272	0.9825
20	0.0196	0.00017171	0.9876
21	0.0241	0.00025488	0.9807
22	0.0255	0.00031587	0.9873
24	0.0274	0.00033617	0.9759
25	0.0190	0.00024605	0.9882

shown in the schematic diagram in Fig. 1. The mean heat transfer rate in the presence of optimized graded metal foam is approximately 8.8% higher than the homogeneous metal foam of 0.95 mean porosity and approximately 1185% higher than that in the presence of pure *n*-octadecane.

Figs. 12 and 13 show the heat transfer rate and a solid height, respectively, in the presence of optimized graded metal foam and homogeneous metal foam of 95% porosity. Fig. 12 shows that the heat transfer rate is higher initially in optimal graded metal foam than homogeneous metal foam, whereas, towards the completion of the solidification process, it is vice-versa. The effective thermal conductivity of PCM-metal foam composite near the isothermal boundary of graded metal foam is higher because of lower porosity near the boundary, which results in a higher heat transfer rate initially. As the solidification front moves away from the isothermal boundary, it transits to higher porosity region (from 92.8% to 95%, and subsequently to 97.2%). The effective thermal conductivity of the last region of graded metal foam is lower than that of homogeneous metal foam. Therefore, towards the completion of the solidification process, the heat transfer rate in optimal graded metal foam is lower than in the homogeneous metal foam.

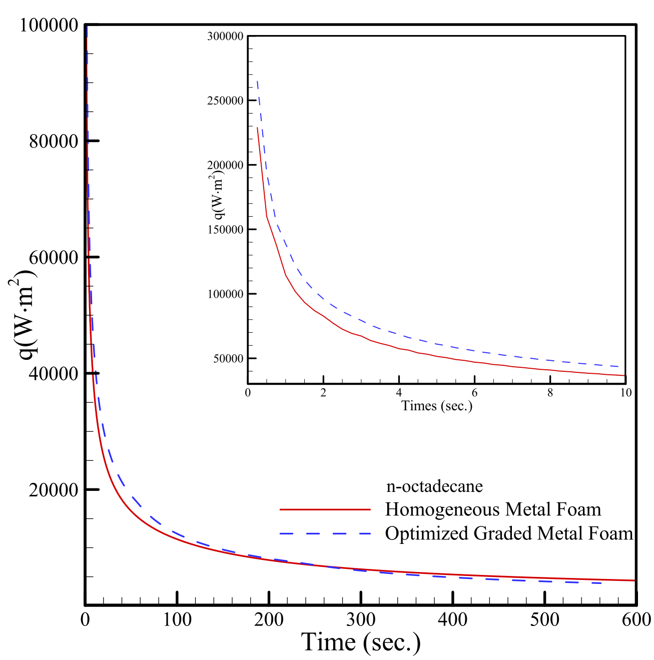

Fig. 12. Heat Transfer rate of TES system filled with n-octadecane in the presence of homogeneous and optimized 3-segment graded metal foams having mean porosity of 0.95.

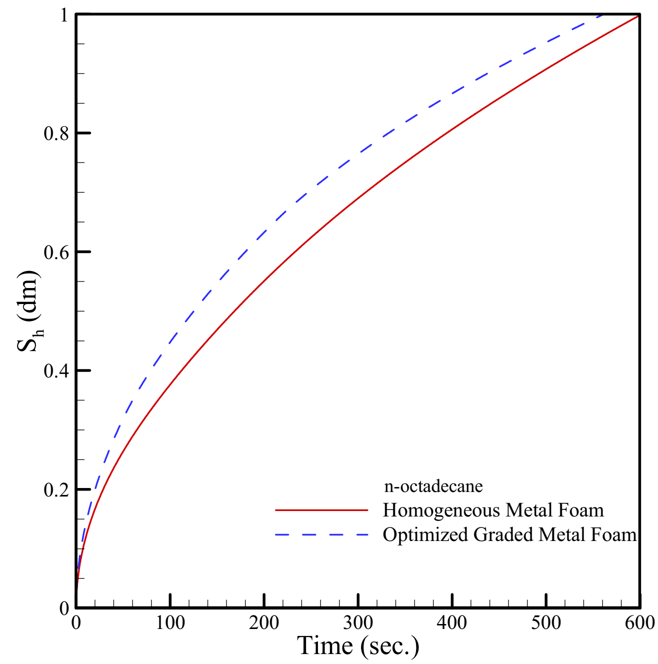

Fig. 13. The progress of solidification height of *n*-octadecane in presence of homogenous and optimized 3-segment graded metal foams respectively.

However, the mean heat transfer rate is approximately 8.8% higher in optimized graded metal foam than the homogeneous metal foam of the same mean porosity. Fig. 13 shows the progress of solidification height with time is initially higher in optimized graded metal foam, whereas it is vice-versa towards completion of the solidification process. The rationale for different progress rate of solidification height compared to uniform metal foam at different stages has been discussed for Fig. 11. However, the solidification process completes in approximately 7% less time compared to uniform metal foam, rather than 5.5% less time as observed for 2-layer graded metal foam. This is primarily because of higher mean heat transfer rate for 3-layer graded metal foam than 2-layer graded metal foam, as observed from Figs. 10 and 12.

The heat transfer augmentation upon employing optimized graded metal foam with two segments is 6.75% compared to single homogeneous metal foam, which further increases to 8.8% upon employing optimized graded metal foam with three segments. However, the increase in heat transfer augmentation is a mere 2.05% upon increasing from two to three segments, compared to 6.75% upon increasing from one to two segments. Therefore, it is evident that the influence of graded metal foam is approaching asymptotic value, and a further increase in the number of segments of graded metal foam will have a limited effect on heat transfer rate. Therefore, in the present study, graded metal foams with more than three segments have not been analyzed.

4. Conclusion

A numerical model based on the Enthalpy-Porosity technique has been developed to study the phase change process in the presence of different graded metal foams. Numerical analyzes have been conducted employing different graded metal foams, of which 80% results have been employed to train the ANN model and the remaining 20% for testing. A back-propagation feed-forward ANN model has been developed to estimate heat transfer for different graded metal foams, which Genetic algorithm utilizes to quantify the potential of different graded metal foams and find optimum graded metal foam porosity distribution. The findings of the present study are:

- The optimal porosity distribution of graded metal foam is independent of the dimensions of TES systems and isothermal boundary temperature. Moreover, the latent heat capacity of PCM and thermal conductivities of metal foam and PCM have limited influence on optimal porosity distribution.
- The optimal porosity distribution for graded metal foam with two segments is $\varepsilon_1 = 93.7\%$; and $\varepsilon_2 = 96.3\%$ and for graded metal foam with three segments is $\varepsilon_1 = 92.8\%$, $\varepsilon_2 = 95.0\%$, and $\varepsilon_3 = 97.2\%$, where ε_1 is closest to the isothermal wall, having mean porosity of 95%.
- The heat transfer rate increases by 1160% and 1185% upon addition of optimized graded metal foams with two and three segments, respectively, compared to pure *n*-octadecane, representing 6.75% and 8.8% augmentation compared to homogeneous metal foam of 95% porosity.
- The unidirectional melting time reduces by 5.5% and 7% compared to homogenous metal foam upon employing optimized graded metal foam with two and three segments, respectively. Therefore, optimal graded metal foams have the potential to augment heat transfer without sacrificing thermal energy storage capacity or increasing manufacturing costs.

CRediT authorship contribution statement

K Venkateshwar: Conceptualization, Methodology, Software, Investigation, Validation, Formal Analysis, Writing – Original Draft.

S H Tasnim: Instruction, Consultation, Review and Editing.

S A Gadsden: Project Management, Formal Analysis, Review and Editing.

Shohel Mahmud: Supervision, Project Management, Funding Acquisition, Formal Analysis, Writing- Review and Editing.

Declaration of competing interest

The authors declare that they have no known competing financial interests or personal relationships that could have appeared to influence the work reported in this paper.

Acknowledgements

The authors would like to acknowledge the support through the Discovery Grant from NSERC (Natural Sciences and Engineering Research Council) Canada (Funder ID: 10.13039/501100000038).

References

[1] B. Zalba, J.M. Marín, L.F. Cabeza, H. Mehling, Review on Thermal Energy Storage With Phase Change: Materials, Heat Transfer Analysis and Applications 23, 2003, https://doi.org/10.1016/S1359-4311(02)00192-8.
[2] A. Sharma, V.V. Tyagi, C.R. Chen, D. Buddhi, Review on thermal energy storage with phase change materials and applications, Renew. Sust. Energ. Rev. 13 (2009) 318–345, https://doi.org/10.1016/j.rser.2007.10.005.
[3] L.F. Cabeza, A. Castell, C. Barreneche, A. De Gracia, A.I. Fernández, Materials used as PCM in thermal energy storage in buildings: a review, Renew. Sust. Energ. Rev. 15 (2011) 1675–1695, https://doi.org/10.1016/j.rser.2010.11.018.
[4] C.Y. Zhao, Review on thermal transport in high porosity cellular metal foams with open cells, Int. J. Heat Mass Transf. 55 (2012) 3618–3632, https://doi.org/10.1016/j.ijheatmasstransfer.2012.03.017.
[5] N.I. Ibrahim, F.A. Al-Sulaiman, S. Rahman, B.S. Yilbas, A.Z. Sahin, Heat transfer enhancement of phase change materials for thermal energy storage applications: a critical review, Renew. Sust. Energ. Rev. 74 (2017) 26–50, https://doi.org/10.1016/j.rser.2017.01.169.
[6] C.Y. Zhao, W. Lu, Y. Tian, Heat transfer enhancement for thermal energy storage using metal foams embedded within phase change materials (PCMs), Sol. Energy 84 (2010) 1402–1412, https://doi.org/10.1016/j.solener.2010.04.022.
[7] K. Venkateshwar, S.H. Tasnim, H. Simha, S. Mahmud, Empirical correlations to quantify the effect of metal foam on solidification process in constant thermal capacity and constant volume systems, J. Energy Storage 30 (2020), 101482, https://doi.org/10.1016/j.est.2020.101482.
[8] J. Yang, L. Yang, C. Xu, X. Du, Numerical analysis on thermal behavior of solid-liquid phase change within copper foam with varying porosity, Int. J. Heat Mass Transf. 84 (2015) 1008–1018, https://doi.org/10.1016/j.ijheatmasstransfer.2015.01.088.
[9] X. Yang, W. Wang, C. Yang, L. Jin, T.J. Lu, Solidification of fluid saturated in open-cell metallic foams with graded morphologies, Int. J. Heat Mass Transf. 98 (2016) 60–69, https://doi.org/10.1016/j.ijheatmasstransfer.2016.03.023.
[10] A. Kumar, S.K. Saha, Latent heat thermal storage with variable porosity metal matrix: a numerical study, Renew. Energy 125 (2018) 962–973, https://doi.org/10.1016/j.renene.2018.03.030.
[11] Y.B. Tao, Y. You, Y.L. He, Lattice boltzmann simulation on phase change heat transfer in metal foams/paraffin composite phase change material, Appl. Therm. Eng. 93 (2016) 476–485, https://doi.org/10.1016/j.applthermaleng.2015.10.016.
[12] Z. Zhang, X. He, Three-dimensional numerical study on solid-liquid phase change within open-celled aluminum foam with porosity gradient, Appl. Therm. Eng. 113 (2017) 298–308, https://doi.org/10.1016/j.applthermaleng.2016.10.173.
[13] K. Venkateshwar, S.H. Tasnim, H. Simha, S. Mahmud, Effect of spatially varying morphologies of metal foams on phase change process, Therm. Sci. Eng. Prog. 19 (2020), 100667, https://doi.org/10.1016/j.tsep.2020.100667.
[14] J.M. Mahdi, E.C. Nsofor, Multiple-segment metal foam application in the shell-and-tube PCM thermal energy storage system, J. Energy Storage 20 (2018) 529–541, https://doi.org/10.1016/j.est.2018.09.021.
[15] Z. Wang, J. Wu, D. Lei, H. Liu, J. Li, Z. Wu, Experimental study on latent thermal energy storage system with gradient porosity copper foam for mid-temperature solar energy application, Appl. Energy 261 (2020), 114472, https://doi.org/10.1016/j.apenergy.2019.114472.
[16] K. Venkateshwar, S.H. Tasnim, H. Simha, S. Mahmud, Influence of metal foam morphology on phase change process under temporal thermal load, Appl. Therm. Eng. 180 (2020), 115874, https://doi.org/10.1016/j.applthermaleng.2020.115874.
[17] V. Joshi, M.K. Rathod, Thermal transport augmentation in latent heat thermal energy storage system by partially filled metal foam: a novel configuration, J. Energy Storage 22 (2019) 270–282, https://doi.org/10.1016/j.est.2019.02.019.
[18] X. Yang, P. Wei, X. Wang, Y.L. He, Gradient design of pore parameters on the melting process in a thermal energy storage unit filled with open-cell metal foam, Appl. Energy 268 (2020), 115019, https://doi.org/10.1016/j.apenergy.2020.115019.
[19] L. Gosselin, M. Tye-gingras, F. Mathieu-potvin, International journal of heat and mass transfer review of utilization of genetic algorithms in heat transfer problems, Int. J. Heat Mass Transf. 52 (2009) 2169–2188, https://doi.org/10.1016/j.ijheatmasstransfer.2008.11.015.
[20] Y. Xu, Z.J. Zheng, C. Yang, X. Cai, Intelligent optimization of horizontal fins to improve the melting performance of phase change materials in a square cavity with isothermal vertical wall, J. Energy Storage 44 (2021), 103334, https://doi.org/10.1016/j.est.2021.103334.
[21] R. Baby, C. Balaji, Thermal optimization of PCM based pin fin heat sinks : an experimental study, Appl. Therm. Eng. 54 (2013) 65–77, https://doi.org/10.1016/j.applthermaleng.2012.10.056.
[22] P.K. Kadiyala, H. Chattopadhyay, Optimal location of three heat sources on the wall of a square cavity using genetic algorithms integrated with artificial neural networks, Int. Commun. Heat Mass Transf. 38 (2011) 620–624, https://doi.org/10.1016/j.icheatmasstransfer.2011.03.018.
[23] P.R. Chakraborty, Enthalpy porosity model for melting and solidification of pure-substances with large difference in phase specific heats, Int. Commun. Heat Mass Transf. 81 (2017) 183–189, https://doi.org/10.1016/j.icheatmasstransfer.2016.12.023.
[24] A. Bhattacharya, V.V. Calmidi, R.L. Mahajan, Thermophysical properties of high porosity metal foams, Int. J. Heat Mass Transf. 45 (2002) 1017–1031, https://doi.org/10.1016/S0017-9310(01)00220-4.
[25] S. Feng, Y. Zhang, M. Shi, T. Wen, T.J. Lu, Unidirectional freezing of phase change materials saturated in open-cell metal foams, Appl. Therm. Eng. 88 (2015) 315–321, https://doi.org/10.1016/j.applthermaleng.2014.09.055.